Extraction and Physicochemical Characterization of Microcrystalline Cellulose from Oil Palm Empty Fruit Bunches

Nur Adriana Mohd Nor Azam[1], Chong Hui Min[1], Abdorreza Mohammadi Nafchi[2], Nor Hakimin Abdullah[3] and Wan Nazwanie Wan Abdullah[1]*

[1]School of Chemical Sciences, Universiti Sains Malaysia, 11800 Penang, Malaysia
[2]Food Technology Division, School of Industrial Technology, Universiti Sains Malaysia, 11800 Penang, Malaysia
[3]Advance Materials Research Centre (AMRC), Faculty of Bioengineering and Technology, Universiti Malaysia Kelantan, 17600 Jeli, Kelantan, Malaysia
*Corresponding author (e-mail: wanazwanie@usm.my)

Microcrystalline cellulose (MCC) is a valuable biopolymer widely used in pharmaceutical, food, and packaging industries due to its biodegradability and functional properties. This study aimed to extract and characterize the physicochemical properties of MCC derived from oil palm empty fruit bunches (OPEFB), an abundant agricultural residue. The extraction process was carried out through an alkaline pretreatment, followed by acid hydrolysis to isolate cellulose and reduce crystallite size. The produced MCC was characterized using Fourier-transform infrared spectroscopy (FTIR), thermogravimetric analysis (TGA), X-ray diffraction (XRD), and field emission scanning electron microscopy with energy-dispersive X-ray spectroscopy (FESEM-EDX). The results indicate that the MCC achieved a crystallinity index of 64.1% and exhibited a rod-like morphology. The TGA curves revealed weight loss in the temperature range of 120°C to 432°C, indicating the thermal degradation of cellulose and hemicellulose, followed by further decomposition up to 900°C. These findings suggest that MCC derived from OPEFB possesses physicochemical properties comparable to those of conventional cellulose sources, making it a promising sustainable alternative. This study highlights the potential of utilizing OPEFB as an eco-friendly raw material for MCC production, in line with waste valorization and circular economy initiative.

Keywords: Microcrystalline cellulose (MCCs); Oil palm empty fruit bunches (OPEFB); extraction

Received: December 2024; Accepted: April 2025

According to the U.S. Department of Agriculture (USDA), Malaysia, a leading global palm oil producer and exporter, contributed 24% to global palm oil production and 32% to global palm oil exports in 2023. The expanding palm oil industry has generated huge amounts of oil palm empty fruit bunch (OPEFB) waste during the milling process of crude palm oil (CPO). Moreover, oil palm is recognized as one of the most economically feasible oil crops cultivated in tropical countries, such as in West Africa and South-East Asia, owing to its valuable oil-producing fruits [1].

OPEFB is therefore typically considered an underutilized by-product of the palm oil industry. However, the OPEFB fiber exhibits positive attributes including high specific strength with low density, affordability, superior electrical and thermal insulating properties, and sustained viability [2]. Numerous studies on oil palm biomass waste management have been conducted in recent years to minimize the wastage of natural resources by converting OPEFB into biomass-based products such as biofertilisers [3], pulp, paper, construction materials, char, activated carbon, and nano carbon production [4]. Since OPEFB waste is rich in cellulose content, it can be transformed into microcrystalline cellulose (MCC), which is gaining popularity for its potential as a valuable reinforcement in polymeric composite materials, thereby contributing to natural resource conservation and offering an alternative solution for OPEFB waste management [5].

Microcrystalline cellulose (MCC), a unique and abundant cellulose derivative, is a fine, white, odorless, crystalline powder obtained by partially hydrolyzing the amorphous regions of natural cellulose. This versatile material has a wide range of industrial applications, including those in the food and pharmaceutical sectors [6]. MCC's advantageous properties, including high surface area, non-toxicity, biodegradability, and biocompatibility, render it an ideal component for various industries [7]. Depending on the preparation method and cellulose source, MCC typically exhibits a diameter of approximately 50 μm, lengths ranging from 100 to 1000 μm, and crystallinity index values between 55% and 80% [8]. However, the main issue with natural materials is that they are hydrophilic, which makes it difficult to adhere to a hydrophobic polymer matrix. Furthermore, natural fibers demonstrate low moisture resistance, resulting in significant water absorption, poor mechanical properties, and compromised dimensional

stability. Alkali treatment is commonly employed to enhance fiber-matrix adhesion in single fibre and fibre/polymer matrix composites, thereby improving their mechanical performance. While MCC is traditionally derived from wood pulp and cotton, alternative sources such as agricultural residues offer a more sustainable and cost-effective approach. Oil palm empty fruit bunches (OPEFB), an abundant by-product of the palm oil industry, represent a promising raw material for MCC production due to their high cellulose content and renewability. This study aims to fill a critical gap in existing research by demonstrating the advantages of MCC derived from OPEFB over conventional sources, particularly in terms of sustainability, cost-effectiveness, and comparable physicochemical properties. Unlike wood-based MCC, which is associated with deforestation, OPEFB utilization supports waste management and circular economy initiatives by converting agro-industrial residues into high-value products. Furthermore, the physicochemical characterization of OPEFB-derived MCC highlights its potential industrial applications, reinforcing its viability as an eco-friendly alternative in biopolymer production.

Thus, this study revolved around the isolation of cellulose and MCC from OPEFB through combined alkaline and hydrogen peroxide pretreatment and acid hydrolysis. As MCC surfaces have a fair amount of -OH groups, they promote surface modification and increase their applications in industry without having any harmful impacts. Various analytical technologies were used to characterize the cellulose and MCC.

MATERIALS AND METHODS

Chemicals and Materials

Fresh OPEFB waste was collected from an oil palm plantation in Penang. Sodium hydroxide (NaOH) pellets were obtained from Fisher Scientific Company. Hydrogen peroxide (H_2O_2) and sulfuric acid (H_2SO_4) solutions of analytical reagent (AR) grade were obtained from QRëC Asia Sdn. Bhd.

Extraction of Cellulose from Raw OPEFB

The collected raw OPEFB waste was rinsed with distilled water four times to remove dust particles and dried in the oven at 60ºC for 12 hours. Subsequently, the dried OPEFB was ground into small pieces (approximately 0.5 cm to 1 cm in size) using a grinder. Approximately 20 g of ground OPEFB was added into a 250 mL beaker containing a 30% NaOH solution (45 g of NaOH pellets dissolved in 150 mL of distilled water). The mixture was then heated at 90°C for 3 hours with constant stirring. Afterwards, the mixture was filtered using a vacuum filtration setup. The collected precipitate underwent a second alkali treatment with a 10% NaOH solution for 1 hour at 80°C with constant stirring. The bleaching process was carried out using a combined alkaline and H_2O_2 treatment, during which the precipitate was continuously stirred and heated in a 3% H_2O_2 solution under alkaline conditions at 75°C for 2 hours. The solution's pH was adjusted to 8–9 by adding drops of 10% NaOH solution. Afterward, the whitish cellulose was filtered and washed with distilled water until the filtrate reached a pH of 5–6. Finally, the cellulose was dried in the oven at 60°C until a constant weight was achieved [9].

Extraction of MCC from OPEFB Cellulose

The preparation of microcrystalline cellulose (MCC) was done via an acid hydrolysis method adopted from the procedure suggested by Nurul Syarima Nadia et al. 0. Firstly, 2 g of dried cellulose was added gradually into a beaker containing 17.5 mL of 50% H_2SO_4 solution with constant stirring for 30 minutes at room temperature. Then, 87.5 mL of cold distilled water was added to the mixture to terminate the reaction. The centrifugation of the mixture was performed at 4,000 rpm for 10 minutes and repeated four times. After each centrifugation, the supernatant was discarded to remove H_2SO_4. The suspension was collected and transferred to dialysis tubes (20,000 Da) for the dialysis process. The suspension was dialyzed against 1000 ml of distilled water and equilibrated until pH 6-7. The suspension was ultrasonicated in an ice bath at 20 kHz for 10 mins to avoid overheating and disperse the microcellulose. Lastly, the suspension was freeze-dried to get the MCC.

Characterization of OPEFB Cellulose and MCC

The functional groups of raw OPEFB, OPEFB cellulose, OPEFB MCC, and commercial MCC were analyzed using Fourier-transform infrared (FTIR) spectroscopy with the attenuated total reflectance (ATR) technique (Perkin-Elmer System 2000 spectrometer) in the range of 4000 cm^{-1} to 600 cm^{-1}. The thermal stability of OPEFB cellulose and MCC was characterized by thermogravimetric analysis (TGA, Perkin-Elmer Thermal Analyzer STA 6000). The surface morphology and elemental composition of the extracted OPEFB cellulose and MCC were examined using field emission scanning electron microscopy coupled with energy-dispersive X-ray spectroscopy (FESEM-EDX) (Quanta FEG 650, Fei). X-ray diffraction (XRD) analysis was performed on OPEFB cellulose and cellulose nanocrystals (CNC) to determine the crystallinity of both samples using Cu-Kα radiation (λ = 1.54180 Å) at 40 kV and 40 mA. The diffraction pattern for each sample was recorded at an angular incidence over a 2θ range of 10°–50° with a step size of 0.02° min^{-1}. The crystallinity index (CrI) of both samples was calculated using the following formula:

$$\%\ \text{of CrI} = \frac{I_{\text{cry}}}{I_{\text{t}}} \times 100\%$$

where I_t is the total area under the XRD curve and I_{cry} is the area under the crystalline peaks 0.

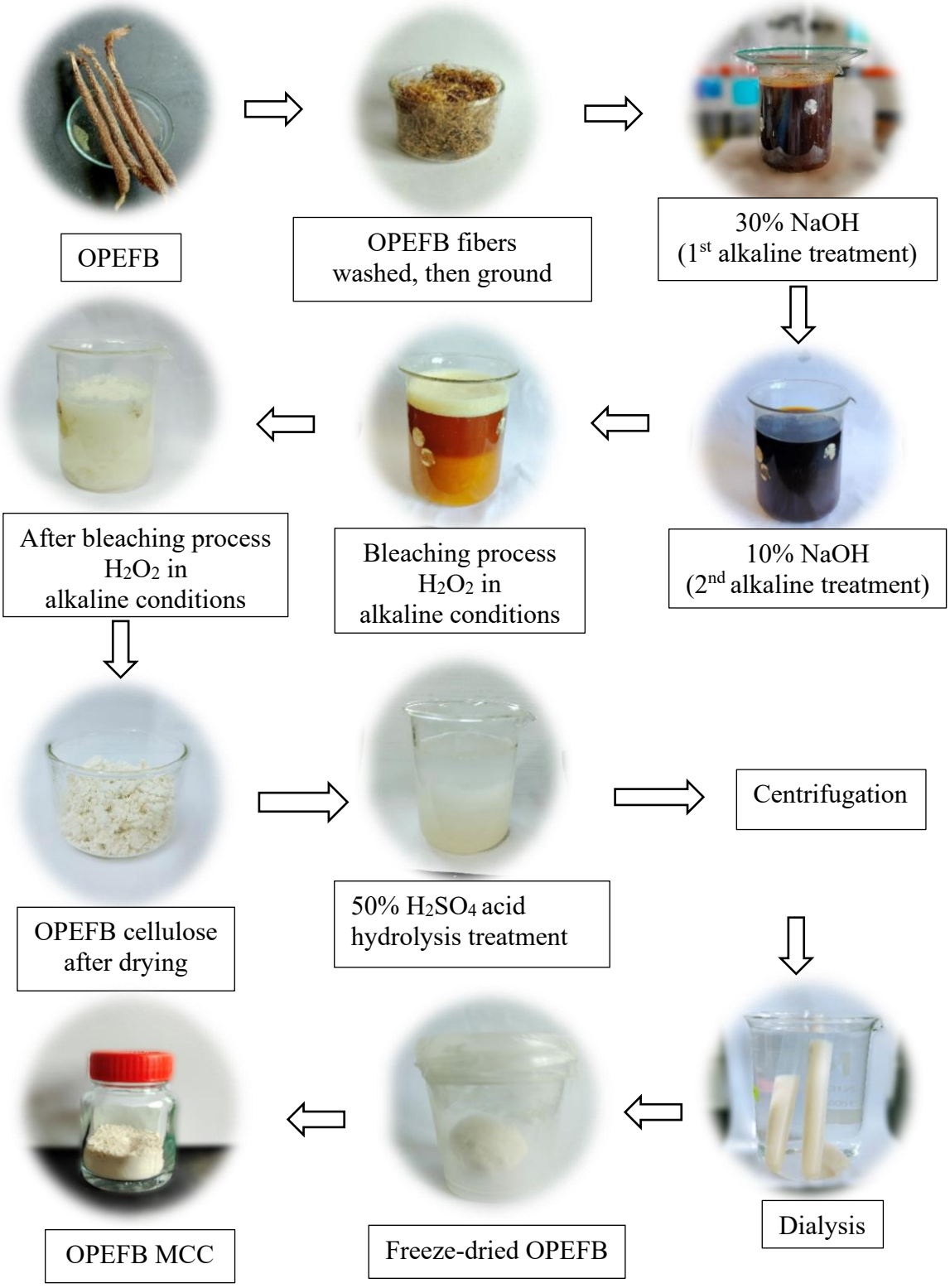

Figure 1. Overview of the extraction of MCC from OPEFB.

RESULTS AND DISCUSSION

Attenuated Total Reflectance-Fourier Transform Infrared (ATR-FTIR) Spectroscopy Analysis

FTIR analyses were performed on raw OPEFB, OPEFB cellulose, OPEFB MCC, and commercial MCC to determine changes in specific functional groups before and after a series of treatment processes and to compare the FTIR spectra of extracted MCC with commercial MCC. The FTIR analyses revealed the absence of certain peaks in the spectra of both OPEFB cellulose and OPEFB MCC, attributed to the gradual removal of lignin and hemicellulose during alkaline and acid treatments. This analysis elucidates the impact of chemical treatment on the structure of raw OPEFB and assesses the effectiveness of MCC isolation by comparing the spectra of OPEFB MCC and commercial MCC.

Referring to the FTIR spectra of all four samples in Figure 2, each spectrum exhibits similar peaks at specific wavenumbers, reflecting the chemical structure of cellulose and aligning with results reported by Ng et al. (2021) [11]. Specifically, a broad absorption peak at 3333 cm^{-1} and an absorption peak at 2900 cm^{-1}, corresponding to the O-H stretching vibration and asymmetric C-H stretching vibration, respectively [11-14]. These two peaks are retained in the spectrum of OPEFB MCC and become sharper and narrower after a series of chemical treatments, indicating that the cellulose components remain intact throughout the process and providing insights into the crystallinity of MCC [5].

The weak absorption bands observed near 1645 cm^{-1}, which correspond to the symmetrical C=C aromatic ring stretching vibration of lignin, were observed in the spectrum of OPEFB MCC after bleaching and acid hydrolysis [15]. The symmetrical CH_2 bending vibration and the bending variations of C–H and C–O groups in cellulose components are shown in the four spectra at 1429 cm^{-1} and 1315 cm^{-1}, respectively [11]. The absorption band at 1160 cm^{-1} in the raw OPEFB spectrum, representing the out-of-plane C–O stretching vibration in lignin, disappeared after the bleaching process, confirming that delignification was successful [12]. After the bleaching and acid hydrolysis processes, a sharper absorption band was observed at 1030 cm^{-1}, attributed to the C=O and C–O stretching vibrations of the carboxylate group, while the absorption band at 897 cm^{-1} is attributed to the β-glycosidic linkages between glucose units in cellulose, comprising of C–H and O–H bendings, respectively [13]. Notably, the extracted MCC exhibits a weaker –OH stretching band. The lower intensity of the –OH stretching band in the extracted MCC suggests reduced hydrogen bonding, which may result in lower moisture absorption compared to commercial MCC. This characteristic is advantageous in packaging applications where moisture resistance is critical.

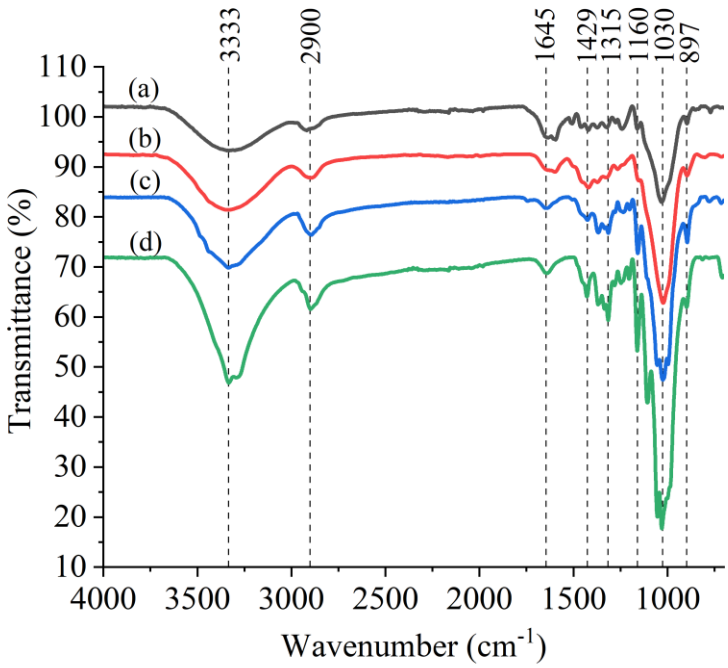

Figure 2. FTIR spectra of (a) raw OPEFB, (b) OPEFB cellulose, (c) OPEFB MCC, and (d) commercial MCC.

Thermal Gravimetric (TGA) Analysis

Thermogravimetric (TGA) and derivative thermogravimetric (DTG) analyses were performed to study the thermal properties of the extracted cellulose and OPEFB MCC, as shown in Figures 3 and 4. The change in sample weight with temperature was evaluated using a TGA thermogram, whereas the rate of weight loss against temperature was determined using a DTG thermogram.

Based on Figure 3, the extracted cellulose and MCC underwent three stages of thermal decomposition. An initial weight loss of 4.470% was recorded for the extracted cellulose sample at temperatures ranging from 29.69°C to 152.78°C, while the first decomposition of the MCC sample occurred at temperatures ranging from 29.62°C to 128.14°C with a weight loss of 4.996%. Moisture evaporation accounts for the minor weight losses (<5%) [16].

During the second stage of thermal decomposition, 67.329% of the cellulose sample degraded at temperatures ranging from 152.78°C to 397.36°C, whereas approximately 76.739% of the MCC sample degraded at temperatures ranging from 128.14°C to 431.73°C. Both cellulosic components experienced greater weight loss during this stage, attributed to decarboxylation, dehydration, decomposition, and depolymerization of glycosyl units in cellulose [17]. A higher weight loss was observed in the MCC sample compared to the cellulose sample, due to the degradation of acidic sulfate groups introduced into MCC through acid hydrolysis [11].

In the final stage, thermal degradation of both extracted cellulose and MCC reached equilibrium, with weight losses of 21.369% for cellulose (at temperatures from 397.36°C to 891.61°C) and 12.875% for MCC (at temperatures from 431.73°C to 894.34°C). The decomposition of lignocellulosic components into solid residues results in the formation of char after heating [16]. At the end of degradation, 6.640% of the cellulose sample and 5.125% of the MCC sample remained.

According to Figure 4, the maximum degradation temperatures (DTG_{max}) of the extracted cellulose and MCC were 312.15°C and 338.70°C, respectively. This result indicates that the extracted MCC is thermally less stable than the extracted cellulose. The slightly lower thermal stability of MCC is likely due to the acid hydrolysis process. Specifically, the substitution of a more negatively charged sulfate group (from sulfuric acid) for a hydroxy group in the MCC structure may accelerate its decomposition. Additionally, the larger surface area of MCC may facilitate greater heat transfer, further reducing its thermal stability [18,19]. The lower thermal stability can contribute to the biodegradability of MCC-based materials, making them more environmentally friendly [20]. This enhanced biodegradability allows the material to break down more easily in the environment, thereby reducing waste accumulation and supporting green manufacturing practices.

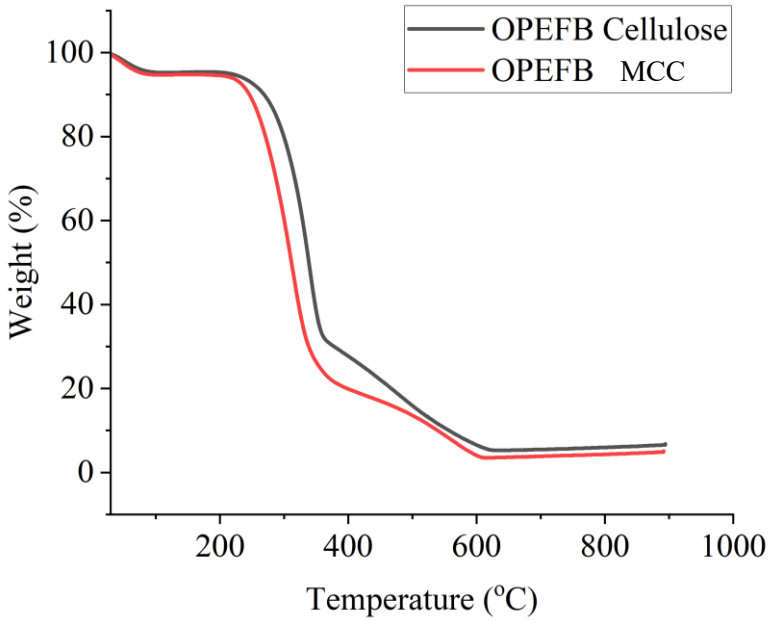

Figure 3. TGA thermograms of OPEFB cellulose and MCC.

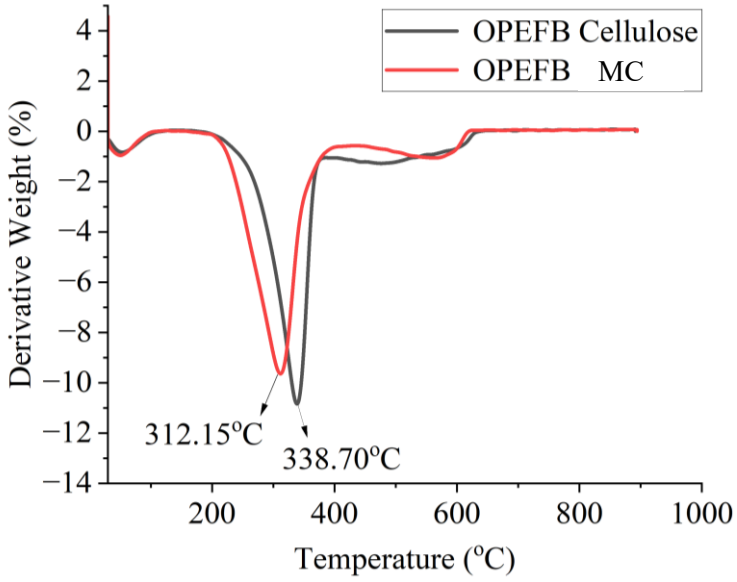

Figure 4. DTG thermograms of OPEFB cellulose and MCC.

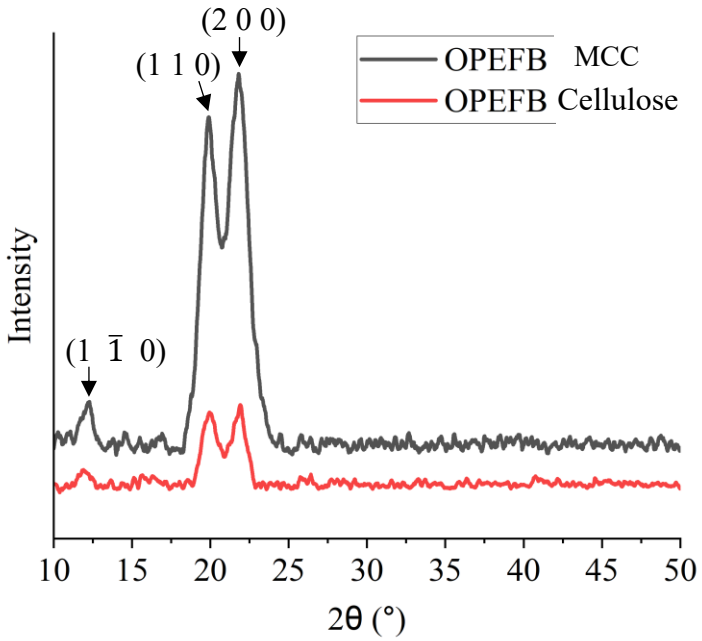

Figure 5. XRD patterns of OPEFB cellulose and MCC.

X-ray Diffraction (XRD) Analysis

The XRD patterns of the extracted OPEFB cellulose and cellulose nanocrystals (CNC) are shown in Figure 5. Both OPEFB cellulose and CNC exhibited crystalline peaks at 12.16°, 19.89°, and 21.77°, corresponding to the (1 $\bar{1}$ 0), (1 1 0), and (2 0 0) crystal planes, respectively. Based on the diffraction patterns, the extracted OPEFB MCC exhibits a mercerized cellulose II crystal structure, as a result of strong alkali treatment during its extraction [21, 22]. The crystallinity index (CrI) values calculated for OPEFB cellulose and MCC were 37.20% and 64.1%, respectively. The CrI of the extracted MCC of 64.1% is comparable to values reported in recent studies. For example, Gapsari et al. (2024) [23] reported a CrI of 68% for MCC extracted from Alpine galanga, whereas Ismail et al. (2021) [24] obtained 51% using a different extraction method. The significant increase in the crystallinity index of MCC after acid hydrolysis is attributed to the effective removal of amorphous regions. Acid hydrolysis of cellulose results in an enhanced crystallinity in the (2 0 0) plane by dissolving amorphous domains and cleaving

glycosidic linkages hydrolytically, thereby generating individual crystallites with a higher CrI [11].

Field Emission Scanning Electron Microscopy-energy Dispersive X-ray (FESEM-EDX) Analysis

The surface morphology of both OPEFB cellulose and OPEFB MCC was examined using FESEM at magnifications of 1000× and 5000×. Raharjo et al. (2023) stated that the flake-like morphology of MCC—with its uneven shape and potential for good interfacial adhesion—contributes to improved mechanical properties in polymer composites by effectively filling voids, enhancing stress transfer, and ultimately increasing the overall strength and stiffness of the material [25]. As shown in Figure 6(ii), the OPEFB cellulose exhibits an elongated fibrous structure with a diameter ranging from 6.391 µm to 7.560 µm, whereas the OPEFB MCC displays a shorter rod-like shape with a diameter ranging from 3.964 µm to 4.824 µm. Additionally, the rod-like shape enhances dispersibility in both aqueous and non-aqueous systems, making it suitable for pharmaceutical formulations—such as tablet binders and drug carriers—where uniform distribution is essential for consistent drug release. Nevertheless, the size of the obtained OPEFB MCC did not match the previously reported diameter of 50 µm, as this depends on the preparation method and cellulose source [8]. This discrepancy is likely due to the long hydrolysis time and low reaction temperature. The acid hydrolysis process cuts the long fibrous cellulose into shorter segments and reduces their diameter; however, this change is not clearly visible in the image due to the agglomeration of MCC. Freeze-dried MCC tends to agglomerate because of the large surface area of nanocrystals, which induces strong intermolecular interactions [26]. Moreover, the addition of small amounts of dispersants, such as surfactants or polymers, may help maintain the separation of MCC particles during the freeze-drying process [27]. The removal of non-cellulosic components after hydrolysis can be confirmed by the reduction in diameter and improved smoothness of the MCC surface [28].

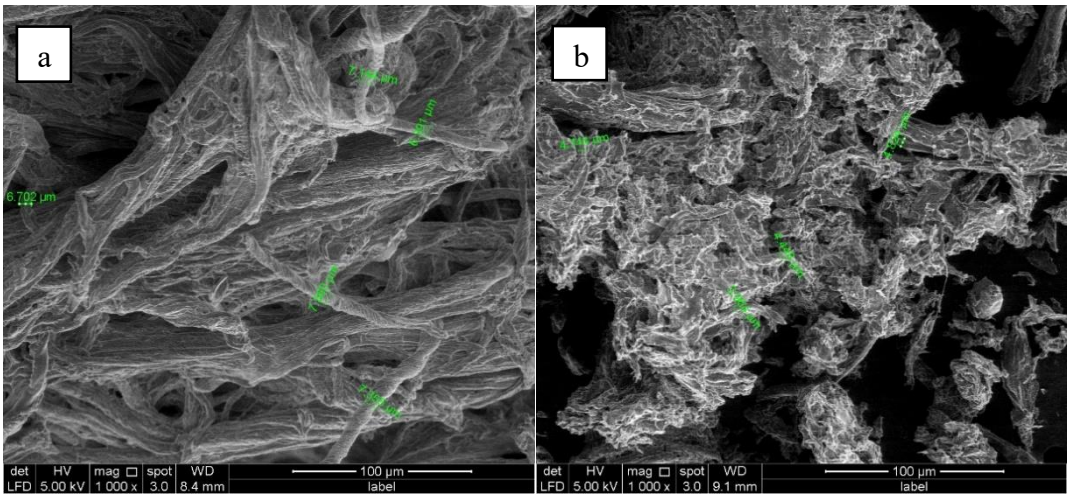

Figure 6(i). FESEM images of (a) OPEFB cellulose and (b) OPEFB MCC at 1000× magnification.

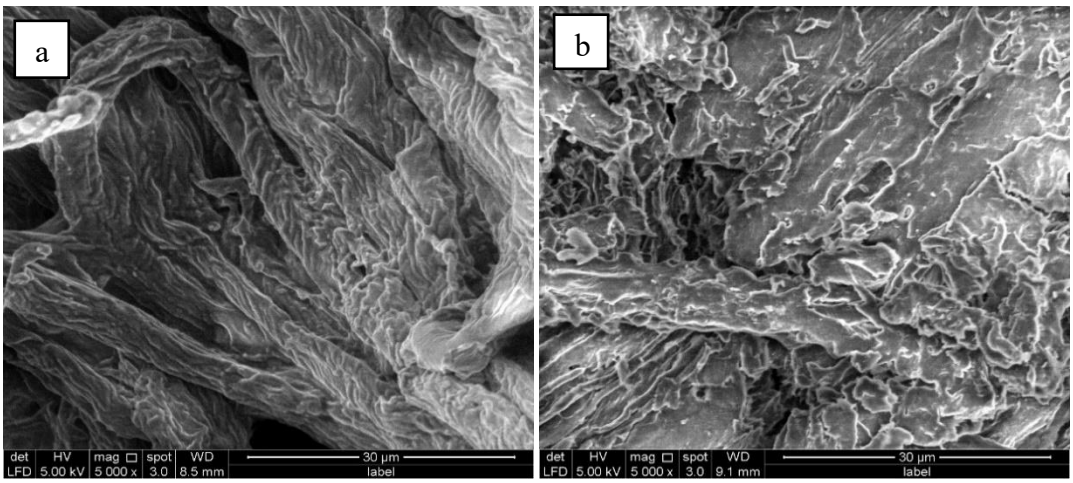

Figure 6(ii). FESEM images of (a) OPEFB cellulose and (b) OPEFB MCC at 5000× magnification.

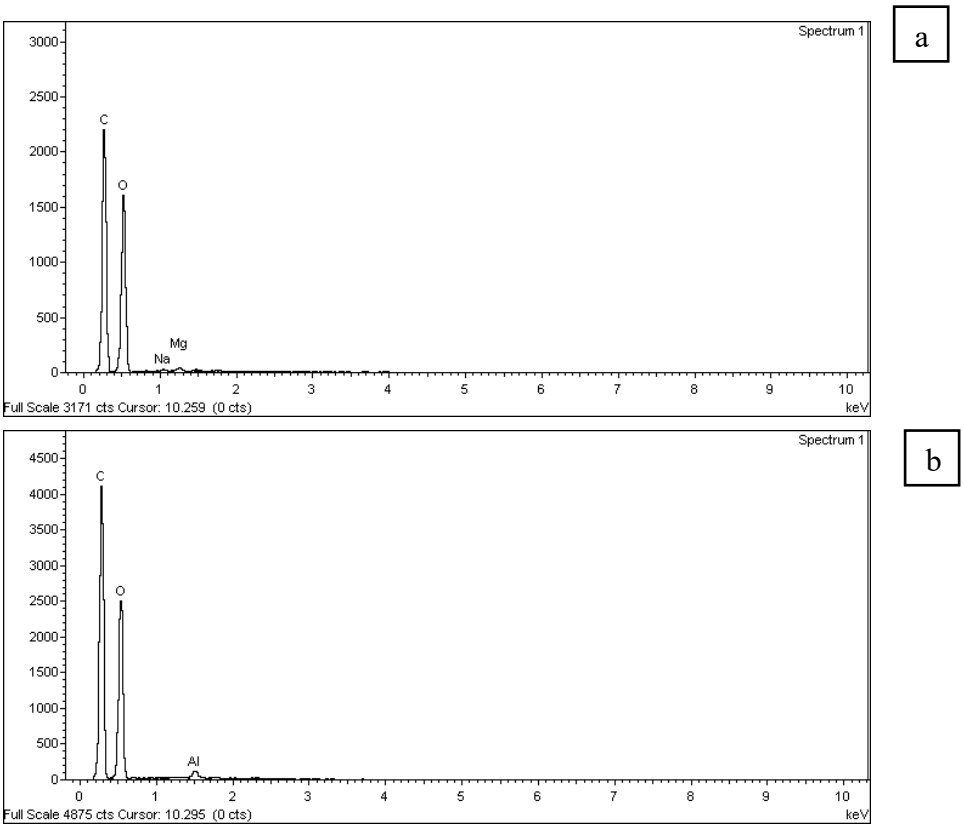

Figure 7 EDX spectra of (a) OPEFB cellulose and (b) OPEFB MCC.

The elemental composition of the samples was analyzed using EDX analysis. Figures 7(a) and (b) display the EDX spectra of both OPEFB cellulose and MCC, showing that the primary constituents are carbon (C) and oxygen (O). A few minor peaks corresponding to sodium (Na), magnesium (Mg), and aluminium (Al) detected in both spectra may be attributed to impurities present on the stub during sample preparation. The carbon contents in OPEFB cellulose and MCC were 48.81% and 51.78%, respectively, while the oxygen contents were 50.56% and 47.32%, respectively. Thus, the weight percentage of C in OPEFB MCC increased by 2.97%, whereas the weight percentage of O decreased by 3.24% compared to OPEFB cellulose. These compositional changes are likely due to the removal of non-cellulosic components (e.g., hemicellulose and lignin), which typically have a lower carbon content, during the acid hydrolysis process, thereby producing a more purified MCC, in agreement with previous findings by Rasheed et al. [29]. Moreover, the absence of significant non-cellulosic components—such as lignin and hemicellulose—improves thermal stability and chemical reactivity, making MCC an ideal candidate for biodegradable packaging applications.

CONCLUSION

In conclusion, cellulose and MCC were successfully extracted from OPEFB. Based on the results, the hydrolysis process cleaved the cellulose into smoother and shorter rod-like segments, reducing the diameter of MCC to 3.964–4.824 μm and increasing its crystallinity index to 64.1%. This study demonstrates the efficiency of the extraction method in producing high-purity MCC with a rod-like morphology and desirable physicochemical properties, thereby confirming its potential for industrial applications. Future work should focus on optimizing the pretreatment processes to achieve nanoscale MCC for advanced material applications, as well as on exploring additional sustainable agricultural residues as alternative cellulose sources. Due to its barrier properties, biodegradability, and reinforcement capabilities, MCC is an excellent candidate for sustainable packaging, particularly in the food and pharmaceutical industries.

ACKNOWLEDGEMENT

The authors are grateful for the financial support from the Ministry of Higher Education Malaysia under the Fundamental Research Grant Scheme

(FRGS), Project Code: FRGS/1/2020/STG04/USM/03/2; and University Sains Malaysia under the Special (Matching) Short-Term Grant, Project No: 304/PKIMIA/ 6315704.

REFERENCES

1. Noah, A. S. (2022) Oil Palm Empty Fruit Bunches (OPEFB) – alternative fibre source for paper-making. In: Kamyab, H., Ed., *Elaeis guineensis*. *In IntechOpen eBooks*, 5-6. https://doi.org/10.5772/intechopen.98256.

2. Abdullah, C. I., Azzahari, A. D., Rahman, N. M. M. A., Hassan, A. & Yahya, R. (2019) Optimizing treatment of oil Palm-Empty Fruit Bunch (OP-EFB) fiber: chemical, thermal and physical properties of alkalized fibers. *Fibers and Polymers*, **20(3)**, 527–537. https://doi.org/10.1007/s12221-019-8492-0.

3. Nadia Farhana Azman, Tomohito Katahira, Nakanishi, Y., Naoya Chisyaki, Uemura, S., Yamada, M., Takayama, K., Oshima, I., Yamaguchi, T., Hara, H. & Yamauchi, M. (2023) Sustainable oil palm biomass waste utilization in Southeast Asia: Cascade recycling for mushroom growing, animal feedstock production, and composting animal excrement as fertilizer. *Cleaner and Circular Bioeconomy*, **6**, 100058–100058. https://doi.org/ 10.1016/j.clcb.2023.100058.

4. Norizan, M. N., Shazleen, S. S., Alias, A. H., Sabaruddin, F. A., Asyraf, M. R. M., Zainudin, E. S., Abdullah, N., Samsudin, M. S., Kamarudin, S. H. & Norrrahim, M. N. F. (2022) Nanocellulose-Based Nanocomposites for Sustainable Applications: A review. *Nanomaterials*, **12(19)**, 3483. https://doi.org/10.3390/nano12193483.

5. Susi, S., Makhmudun Ainuri, Wagiman Wagiman, & Affan, M. (2024) Characterization and Selection of Microcrystalline Cellulose from Oil Palm Empty Fruit Bunches for Strengthening Hydrogel Films. *Journal of Renewable Materials*, 0(0), 1–10. https://doi.org/10.32604/jrm. 2024. 045586.

6. Xiang, L. Y., Mohammed, M. A. P. & Baharuddin, A. S. (2016) Characterisation of microcrystalline cellulose from oil palm fibres for food applications. *Carbohydrate Polymers*, **148**, 11–20. https://doi.org/10.1016/j.carbpol.2016.04.055.

7. Harini, U., Harish, S., Harishankar, A., Buvaneswaran, M. & Sinija, V. (2024) Extraction and characterization of microcrystalline cellulose from wine waste. *Food and Bioproducts Processing*, **144**, 92–101. https://doi.org/10.1016/j.fbp.2024.01.001.

8. Haldar, D. & Purkait, M. K. (2020) Micro and nanocrystalline cellulose derivatives of lignocellulosic biomass: A review on synthesis, applications and advancements. *Carbohydrate Polymers*, **250**, 116937. https://doi.org/10.1016/j.carbpol.2020.116937.

9. Alhamzani, A. G. & Habib, M. A. (2021) Preparation of cellulose nanocrystals from date palm tree leaflets (phoenix dactylifera l) via repeated chemical treatments. *Cellulose Chemistry and Technology*, **55(1-2)**, 33–39. https://doi.org/10.35812/cellulosechemtechnol.2021.55.04.

10. Nurul Syarima Nadia, S., Hartini, A. R., Shaari, D., Norshahidatul Akmar, M. S., Mohamad Azam Akmal, A. B. & Zul Adlan, M. H. (2023) Extraction and Physicochemical Characterization of Micro-crystalline Cellulose from Gigantochloa scortechinii. *Malaysian Journal of Chemistry*, **25(3)**. https://doi.org/10.55373/mjchem.v25i3.323.

11. Ng, L. Y., Wong, T. J., Ng, C. Y. & Amelia, C. K. M. (2021) A review on cellulose nanocrystals production and characterization methods from Elaeis guineensis empty fruit bunches. *Arabian Journal of Chemistry*, **14(9)**, 103339. https://doi.org/10.1016/j.arabjc.2021.103339.

12. Salazar-Bravo, P., Torres-Huerta, A., Domínguez-Crespo, M., Brachetti-Sibaja, S., Licona-Aguilar, A., Rodríguez-Salazar, A. & Willcock, H. (2023) Electrospun PVA membranes reinforced with cellulose nanocrystals and thermally reduced graphene oxide: Thermal, mechanical and UV-protection properties. *Industrial Crops and Products*, **197**, 116614. https://doi.org/10.1016/j.indcrop.2023.116614.

13, Wahab, N. A. (2020) Extraction and characterisation of cellulose from the residue of oil palm empty fruit bunch-xylan extraction. *Journal of Oil Palm Research*. https://doi.org/10.21894/jopr.2020.0052.

14. Shaari Daud, N. S. N. S., Mohd Shohaimi, M. A., Abu Bakar, M. A. A., Mohd Hir, Z. A. & Rafaie, H. A. (2023) Extraction and physicochemical characterization of microcrystalline cellulose from Gigantochloa scortechinii. *Malaysian Journal of Chemistry*, **25(3)**, 323. https://doi.org/10.55373/mjchem.v25i3.323.

15. Jing, S., Shen, S., Peng, X., Pan, H., Wang, C., Wu, B., Li, J., Wu, T. & Xing, Y. (2021) Preparation of a novel solid acid bearing sulfur-containing active groups and evaluation of its activity for cellulose hydrolysis. *Fuel Processing Technology*, **224**, 107004. https://doi.org/10.1016/j.fuproc.2021.107004.

16. Raza, M., Abu-Jdayil, B., Banat, F. & Al-Marzouqi, A. H. (2022) Isolation and Characterization of Cellulose Nanocrystals from Date Palm Waste. *ACS Omega*, **7(29)**, 25366–25379. https://doi.org/10.1021/acsomega.2c02333.

17. Tessema, T. A., Feroche, A. T., Workneh, G. A. & Gabriel, T. (2023) Physicochemical characterization of cellulose and microcrystalline cellulose from Cordia africana Lam. Seeds. *Journal of Natural Fibers*, **20(2)**. https://doi.org/10.1080/15440478.2023.2198278.

18. Al-Dulaimi, A. A. & Wanrosli, W. D. (2016) Isolation and characterization of nanocrystalline cellulose from totally chlorine free oil palm empty fruit bunch pulp. *Journal of Polymers and the Environment*, **25(2)**, 192–202. https://doi.org/10.1007/s10924-016-0798-z.

19. Chieng, B., Lee, S., Ibrahim, N., Then, Y. & Loo, Y. (2017) Isolation and characterization of cellulose nanocrystals from oil palm mesocarp fiber. *Polymers*, **9(8)**, 355. https://doi.org/10.3390/polym9080355.

20. Erdal, N. B. & Hakkarainen, M. (2022) Degradation of cellulose derivatives in laboratory, Man-Made, and natural environments. *Biomacromolecules*, **23(7)**, 2713–2729. https://doi.org/10.1021/acs.biomac.2c00336.

21. French, A. D. (2013) Idealized powder diffraction patterns for cellulose polymorphs. *Cellulose*, **21(2)**, 885–896. https://doi.org/10.1007/s10570-013-0030-4.

22. Ferro, M., Mannu, A., Panzeri, W., Theeuwen, C. H. & Mele, A. (2020) An Integrated approach to optimizing cellulose mercerization. *Polymers*, **12(7)**, 1559. https://doi.org/10.3390/polym12071559.

23. Gapsari, F., Setyarini, P., Harmayanti, A., Puttegowda, M., Arsya, M., Rangappa, S. M., Siengchin, S. (2024) Isolation and extraction of microcellulose from Alpine galanga fiber. *Sustainable Chemistry and Pharmacy*, **42**. 101829. https://doi.org/10.1016/j.scp.2024.101829.

24. Ismail, F., Othman, N. E. A., Wahab, N. A., Hamid, F. A. & Aziz, A. A. (2021) Preparation of microcrystalline cellulose from oil palm empty fruit bunch fibre using steam-assisted acid hydrolysis. *Journal of Advanced Research in Fluid Mechanics and Thermal Sciences*, **81(1)**, 88–98. https://doi.org/10.37934/arfmts.81.1.8898.

25. Raharjo, W. W., Salam, R. & Ariawan, D. (2023) The effect of microcrystalline cellulose on the physical, thermal, and mechanical properties of composites based on cantala fiber and recycled High-Density polyethylene. *Journal of Natural Fibers*, **20(2)**. https://doi.org/10.1080/15440478.2023.2204454.

26. Girard, M., Bertrand, F., Tavares, J. R. & Heuzey, M. (2021) Rheological insights on the evolution of sonicated cellulose nanocrystal dispersions. *Ultrasonics Sonochemistry*, **78**, 105747. https://doi.org/ 10.1016/j.ultsonch.2021.105747.

27. Ghosh, P., Rasmuson, A. & Hudson, S. P. (2023) Impact of additives on drug particles during liquid antisolvent crystallization and subsequent freeze-drying. *Organic Process Research & Development*, **27(11)**, 2020–2034. https://doi.org/10.1021/acs.oprd.3c00204.

28. Kamelnia, E., Divsalar, A., Darroudi, M., Yaghmaei, P. & Sadri, K. (2019) Production of new cellulose nanocrystals from Ferula gummosa and their use in medical applications via investigation of their biodistribution. *Industrial Crops and Products*, **139**, 111538. https://doi.org/10.1016/j.indcrop.2019.111538.

29. Rasheed, M., Jawaid, M., Parveez, B., Zuriyati, A. & Khan, A. (2020) Morphological, chemical and thermal analysis of cellulose nanocrystals extracted from bamboo fibre. International *Journal of Biological Macromolecules*, **160**, 183–191. https://doi.org/10.1016/j.ijbiomac.2020.05.170.